Structure and process-dependent properties of solid-state spun carbon nanotube yarns

2010 J. Phys.: Condens. Matter 22 334221

(http://iopscience.iop.org/0953-8984/22/33/334221)

J. Phys.: Condens. Matter **22** (2010) 334221 (6pp) doi:10.1088/0953-8984/22/33/334221

Structure and process-dependent properties of solid-state spun carbon nanotube yarns

Shaoli Fang[1,3], **Mei Zhang**[2], **Anvar A Zakhidov**[1] **and Ray H Baughman**[1]

[1] The Alan G MacDiarmid NanoTech Institute, University of Texas at Dallas, Richardson, TX 75083, USA
[2] Department of Industrial and Manufacturing Engineering, FAMU-FSU College of Engineering & High-Performance Materials Institute, Florida State University, Tallahassee, FL 32310, USA

E-mail: sfang@utdallas.edu

Received 3 February 2010, in final form 22 April 2010
Published 4 August 2010
Online at stacks.iop.org/JPhysCM/22/334221

Abstract
The effects of processing conditions and apparent nanotube length on properties are investigated for carbon nanotube yarns obtained by solid-state drawing of an aerogel from a forest of multi-walled carbon nanotubes. Investigation of twist, false twist, liquid densification and combination methods for converting the drawn aerogel into dense yarn show that permanent twist is not needed for obtaining useful mechanical properties when nanotube lengths are long compared with nanotube diameters. Average mechanical strengths of 800 MPa were obtained for polymer-free twist-spun multi-walled carbon nanotube (MWNT) yarns and average mechanical strengths of 1040 MPa were obtained for MWNT yarns infiltrated with 10 wt% polystyrene solution. Strategies for increasing the mechanical properties are suggested based on analysis of intra-wall, intra-bundle and inter-bundle stress transfer.

(Some figures in this article are in colour only in the electronic version)

1. Introduction

Carbon nanotubes have been the focus of diverse studies, both fundamental and directed at exploitation of their novel physical properties [1–3]. Commercial synthesis methods produce either carbon single-walled nanotubes (SWNTs) or carbon multi-walled nanotubes (MWNTs) as a soot-like material. The strength and elastic modulus of individual carbon nanotubes in this soot are well known to be exceptionally high, ~37 GPa and ~0.64 TPa, respectively, for about 1.4 nm diameter SWNTs [1, 4, 5]. Relevant for applications needing strong light materials, the density-normalized modulus and strength of individual SWNTs are even more impressive, ~19× and ~54× higher, respectively, than for high strength steel wire. A critical problem hindering applications is the need for methods for high rate assembly of nanotubes into yarns, sheets and other shaped articles that effectively utilize the properties of the individual nanotubes. Since such nanotubes can confer functionalities other than mechanical properties, methods are needed for enhancing the mechanical properties of fibers made of the nanotubes without compromising these other functionalities. Important examples of these other functionalities, which combine with the mechanical functionality to make the fibers multifunctional, are electrical and thermal conductivity, electromechanical actuation and electrical energy storage.

Building on the pioneering results showing that aerogel yarns could be drawn from MWNT forests [6], we have previously reported downsizing ancient twist-based spinning technology for making continuous, densified nanotube yarns from these forests [7]. Such nanotube yarns provide unique properties and property combinations, like extreme toughness, resistance to failure at knots, high electrical and thermal conductivities, high reversible absorption of mechanical energy, up to 13% strain-to-failure, high resistance to creep,

[3] Author to whom any correspondence should be addressed.

retention of strength even when heated in air at 450 °C for 1 h, and very high radiation and UV stability even when irradiated in air. Furthermore, these nanotube yarns can be spun as micron diameter yarns and plied at will to make twofold, fourfold and higher-fold yarns. Other researchers have made important advances in improving and deploying this increasingly popular approach [8–14].

Despite this important progress, the relationship between nanotube yarn properties and component carbon nanotube properties is not fully understood and processing alternatives to twist-based spinning require further exploration. The goal of this study is to obtain a fundamental understanding of the origin of the differences in the properties of individual nanotubes and solid-state spun nanotube yarns and to use this understanding to improve yarn properties. To achieve this ultimate goal, we have related single nanotube properties to that of nanotube yarns, investigated the effects of nanotube length and yarn processing variables on targeted properties, and investigated the properties of carbon nanotube/polymer composites.

2. Experimental details

Three densification methods were used for obtaining high performance MWNT yarns by forest spinning: twist, false twist and liquid densification, as well as combinations thereof. Twist-spun yarns were produced by simultaneously applied draw and twist to ribbons drawn directly from forests of vertically oriented MWNTs [7], which were grown on an iron-catalyst-coated substrate by chemical vapor deposition of acetylene gas [7, 15]. The as-drawn aerogel ribbons (sheets) typically have a density of ∼1.5 mg cm^{-3}, an areal density of ∼1–3 μg cm^{-2} and a thickness of ∼20 μm [15]. The direction of draw was orthogonal to the original nanotube orientation in the forest and parallel to the plane of the substrate. The yarn diameter is controlled by the width of the ribbon from which it is spun and measured using scanning electron microscopy (SEM). Another factor affecting yarn diameter is the areal density of the MWNT ribbon. With fixed width, ribbons with higher areal density produce larger diameter yarns. The helix angle of the twist-spun yarn is directly related to the angle of the spinning wedge, which is controlled by the ratio of twist rate and drawing speed. For yarns with large helix angle (high twist density), tension is maintained during post-spinning sample handling to prevent yarn entanglement.

False twist is basically twisting in one direction followed by inserting an approximately equal twist in the opposite direction, so that the net twist is essentially zero. As a result, nanotubes in false-twisted yarns are aligned in the yarn tensile axis direction. Liquid densification of as-drawn yarns involves imbibing a liquid and subsequent liquid evaporation, which causes the MWNT aerogel to collapse.

Mechanical properties of the yarns were characterized using an Instron Mechanical Tester and gauge lengths between 8 and 10 mm.

3. Results and discussion

Yarn strength and modulus depend upon the degree of stress transfer between nanotube bundles in a yarn, between nanotubes inside a bundle and between walls of a nanotube. We here investigate these dependences for forest-drawn MWNT yarns that comprise ∼12 nm diameter MWNTs containing ∼9 walls, which are highly bundled. The average bundle contains roughly 25 MWNTs and there is wide dispersity in the degree of bundling (from 1 to ∼60 nanotubes in a bundle) [15]. Figure 1 pictures nanotube structure on vastly different dimensional scales, from the individual nanotube to the interconnected structure in the sheet strips that are drawn from the forest, and twist-spun MWNT yarn.

Increasing MWNT length increases the number of times a nanotube bundle can wrap around the yarn circumference and migrate between yarn surface and yarn interior, which increases stress transfer between a nanotube in a bundle and other nanotubes in the yarn, thereby increasing yarn strength. The data in figure 2 shows measured yarn strength as a function of yarns having about the same helix angle (17°–21°) and yarn diameter (5–7 μm). The nanotube length, estimated from the forest height, was from 160 to 390 μm for different yarns. Along with the shown increase in average yarn strength with increasing nanotube length, we also found that the average strain to failure was much lower for the 160 μm long MWNTs (2.5%–4%) than for either the 240 μm long MWNTs (9.3%–12.3%) or the 390 μm long MWNTs (9.3%–10.3%). Correspondingly, average yarn toughness (work-to-break) increased from 6.7 to 22.5 and 17.2 J g^{-1}, with increasing MWNT length in this series. While the only variable changed to produce these different length nanotubes was forest growth time, care must be used in interpreting the functional form of the dependence of these yarn properties on nanotube length (because of possible co-evolution of other variables with growth time, like details of forest structure and increase of contaminants on the nanotube surfaces).

We next investigated the effects of yarn diameter and helix angle on the mechanical strength of twist-spun MWNT yarns. Theory predicts that the ratio of yarn tensile strength (σ_y) to the tensile strength of the component bundles (σ_f) is approximately

$$\sigma_y/\sigma_f \approx \cos^2\alpha(1 - k\,\mathrm{cosec}\,\alpha), \tag{1}$$

where $k = (dQ/\mu)^{1/2}/3L$, α is the helix angle that the component fibers make with the yarn axis, d is the diameter of these fibers, μ is the friction coefficient between fibers, L is the fiber length and Q (the fiber migration length) is the distance along the yarn over which a fiber shifts from the yarn surface to the deep interior and back again [16].

According to the above equation, decreasing yarn diameter should increase yarn strength (over and above the usual volumetric effect of decreasing the probability that critical size defects exist in a given yarn length). To investigate this effect, we kept the yarn helix angle constant (either $\alpha \sim 15°$ or $\alpha \sim 50°$, for low and high degrees of twist, respectively, by varying the width of forest side-wall that is spun and the amount of inserted twist in turns m^{-1} yarn length) for yarn

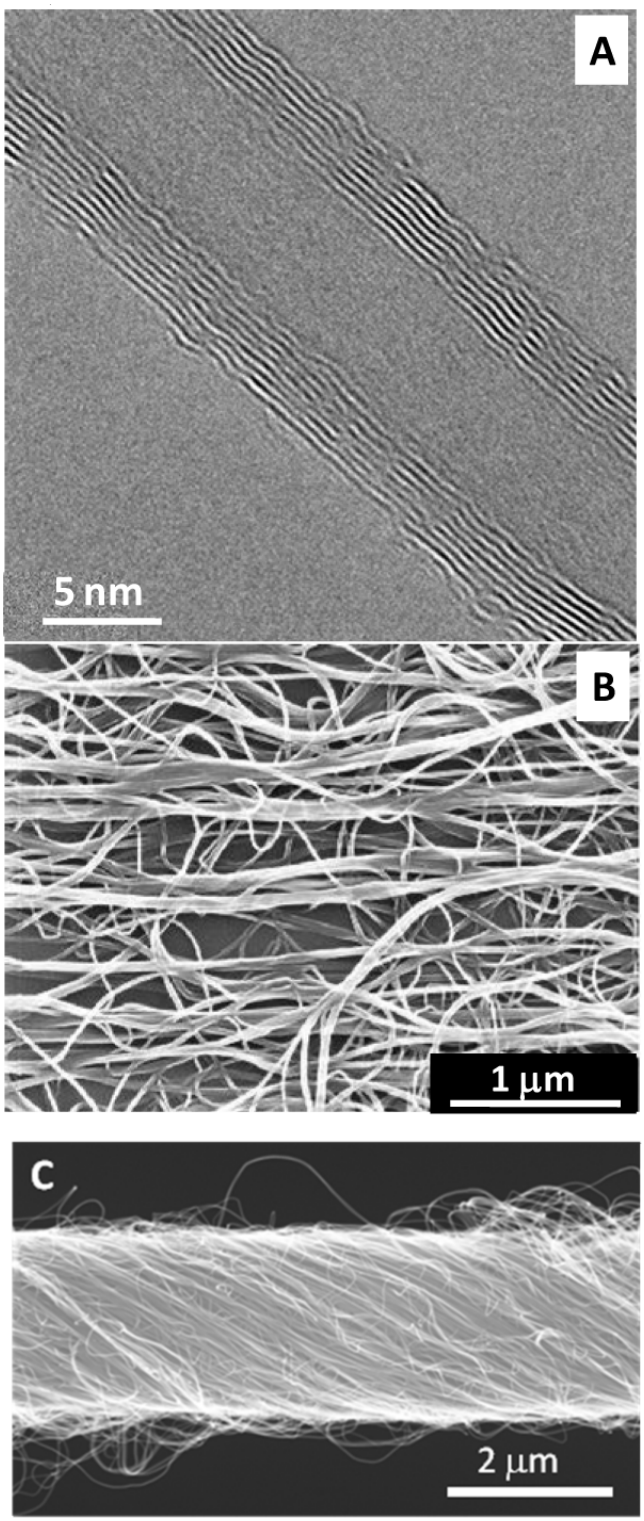

Figure 1. (A) Transmission electron microscope image showing an MWNT from a forest used to produce yarn, (B) an SEM image of a forest-drawn MWNT aerogel sheet strip that can be densified to make a yarn and (C) an SEM image of an MWNT yarn that was twist spun from such an MWNT aerogel sheet strip.

spun from a 350 μm high forest. The results in figure 3 show that yarn strength substantially increases with decreasing yarn diameter, and that the slope of this approximately linear

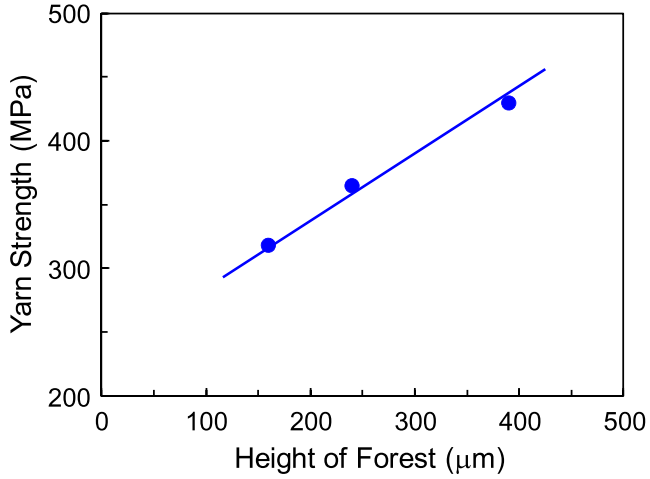

Figure 2. Dependence of the strength of a twist-spun MWNT yarn on forest height for MWNT forests grown by CVD of acetylene gas. All tensile strengths are for yarns with about the same helix angle (17°–21°) and diameter (5–7 μm).

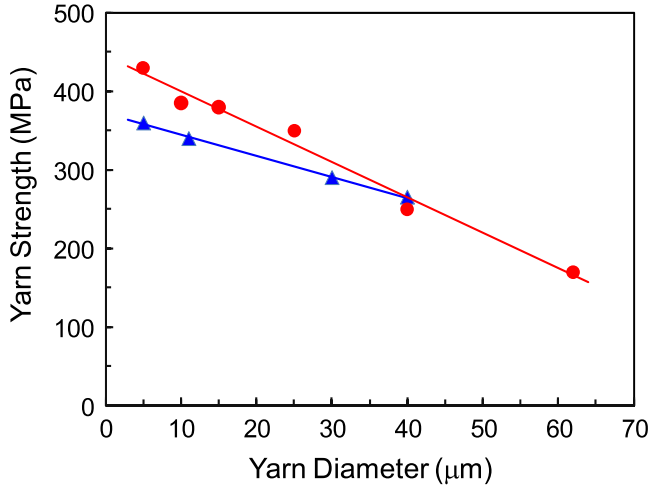

Figure 3. Dependence of yarn tensile strength on yarn diameter for low twist yarns (circles, for helix angle $\alpha \sim 15°$) and high twist yarns (triangles, for helix angle $\alpha \sim 50°$). The forest used for spinning had a height of 350 μm, which is the nominal nanotube length.

dependence is largest for yarns having the smaller helix angle (i.e. least twist). The observed linear dependence of strength on yarn diameter (with negative slope) agrees with equation (1) only if the fiber migration length is proportional to D^2, where D is the yarn diameter. Even in this case the predicted ratio of line slope for 15° bias angle to that for 50° bias angle (4.7) is much larger than that for the figure 3 data (2.1). The observed strain to failure (~10% for $\alpha \sim 15°$ and 11% for $\alpha \sim 50°$) is not very sensitive to yarn diameter.

Figure 4 shows measurement results for the dependence of yarn strength on the helix angle α obtained by twist insertion, which is given by $\tan(\alpha) = \pi T D$, where T is the yarn twist in rotations per yarn length. Yarn diameter D was kept relatively constant at between 18 and 20 μm. Since application of very low twist (corresponding to a helix angle below 10°) results in non-uniform twist and yarn diameter, yarn samples used in

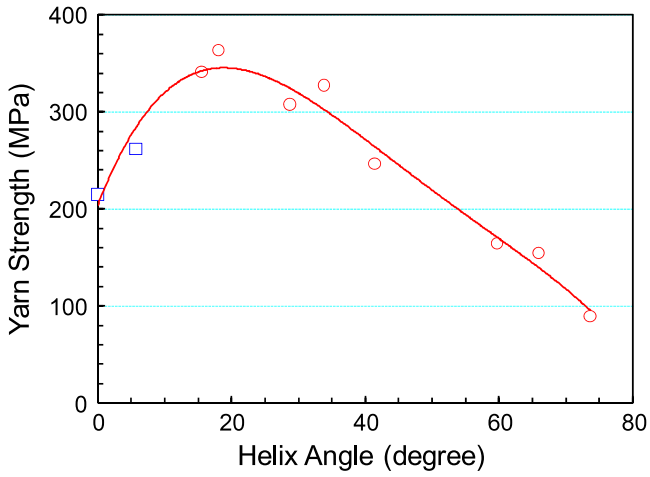

Figure 4. Dependence of yarn tensile strength on yarn helix angle for forest-spun MWNT yarn. Yarns having very low twist (squares) were liquid densified before twist insertion, and the remaining yarns (circles) were twist-spun without any prior treatment. The yarn diameter was kept constant at ∼20 μm. The forest used for spinning had a height of 350 μm, which is the nominal nanotube length.

this angle range were densified by ethanol absorption after the insertion of twist. Figure 4 shows that a peak tensile strength of ∼340 MPa is achievable with a helix angle of ∼20° for this ∼20 μm diameter yarn (much higher strengths result for smaller yarn diameters).

Forest quality for spinning, as well as yarn mechanical properties, depends upon what would be usually considered minor changes in growth conditions (or even change in furnace diameter). By optimizing these conditions (yarn diameter, helix angle, forest height and forest growth conditions), we have obtained an average mechanical strength of 800 MPa for ∼4 μm diameter MWNT yarns that were spun from a 550 μm high forest. Especially considering the low yarn density (∼0.8 g cm^{-3} versus ∼1.7 g cm^{-3} for high strength graphite fibers, like IM6), the high yarn toughness and the absence of significant strength degradation upon yarn knotting [7], this strength is in the useful range.

Why are these mechanical properties so much lower than those of individual small-diameter SWNTs, ∼37 GPa, based on total nanotube cross section for small-diameter nanotubes [4, 5]? The first problem is low stress transfer between outer and inner walls of individual MWNTs. Although Ruoff's group reported high tensile strength for the outer wall of 1–8 μm long MWNTs (12–41 GPa, when normalized to the van der Waals cross section, instead of the much larger total cross section for the nanotube cylinder), their observation of sword-in-sheath rupture indicates that mechanical load is not effectively transferred from the outer wall to the nearest inner wall [17, 18]. The question then becomes: 'How long must be a carbon nanotube before stress can be effectively transmitted from the outer wall to inner walls?' Results for 1.5–20 nm diameter MWNTs show stress transfer from the outer wall to one adjacent inner wall when the MWNT length is one centimeter [19]. Since our presently investigated MWNTs (<550 μm long) are much shorter than a centimeter, these results suggest that only the outer wall of our MWNTs are effective in supporting load. Since this outer nanotube wall is, on average, only about 14.4% of the total weight of the entire MWNT, lack of effective load transfer from the outer wall to even the first inner wall reduces the MWNT specific strength (i.e. strength divided by density) by a factor of ∼7. This strength penalty could be eliminated by transitioning from large-diameter MWNTs to single-wall nanotubes or ultra-long few-walled nanotubes.

Lack of effective stress transfer between outer and inner nanotubes in a bundle is another problem when the lengths of individual nanotubes are not sufficiently long, and this issue becomes especially important when bundle size is large, as it is for the present yarns. Additionally, nanotube bundling decreases the surface-to-volume ratio, which can degrade mechanical strength by decreasing stress transfer between nanotube bundles. (This ratio is ∼12 times larger for a single MWNT than for a bundle of 100 MWNTs.) Consequently, decreasing nanotube bundle size is again noted as another means for increasing strength.

The major increase in strength in going from a highly oriented, forest-drawn nanotube aerogel to a yarn is a result of the ∼500-fold increase in density produced by twist (from ∼1.5 mg cm^{-3} to ∼0.8 g cm^{-3}). In fact, the specific strength of a carbon nanotube aerogel sheet is ∼130 MPa cm^3 g^{-1} and increases to ∼460 MPa cm^3 g^{-1} upon sheet densification (by imbibing and subsequent evaporation of a liquid like methanol). This latter specific strength is only about a factor of two lower than that of the maximum specific yarn strength reported here (1000 MPa cm^3 g^{-1}, corresponding to a yarn strength and density of 800 MPa and 0.8 g cm^{-3}, respectively). Moreover, large permanent twist has the disadvantage, shown in equation (1) and the data of figure 4, of decreasing mechanical strength.

Consequently, we inquired a number of years ago in patent-related research [20] whether or not densification produced by surface tension effects (liquid imbibing and liquid evaporation from untwisted yarn, or a very slightly twisted yarn) or false twist can be used to increase yarn strength. This could be the case if the $k = (dQ/\mu)^{1/2}/3L$ in equation (1) was very small (because of the high friction coefficient μ between fibers, presently largely nanotube bundles) and nanofiber length L is long. The data of figure 4 shows that little twist (i.e. a small helix angle) is needed to maximize strength. Furthermore, the substantial strength obtained for zero helix angle (where the yarn was densified using liquid-based densification) supports the idea that inter-bundle stress transfer can be relatively high even when twist is not inserted). Liquid-based densification of forest-drawn aerogel fibers (narrow aerogel ribbons) results in irregular aerogel collapse to form a densified yarn having non-uniform cross section. We can largely eliminate such irregularities by inserting a very small degree of twist or a false twist before conducting liquid-based densification. Other researchers have utilized this liquid-based densification process for making continuous nanotube yarns with improved mechanical properties [21–23].

Liquid-based densification using a solvent that contains dissolved polymer can be used to increase stress transfer between nanotube bundles in yarns. The solution used

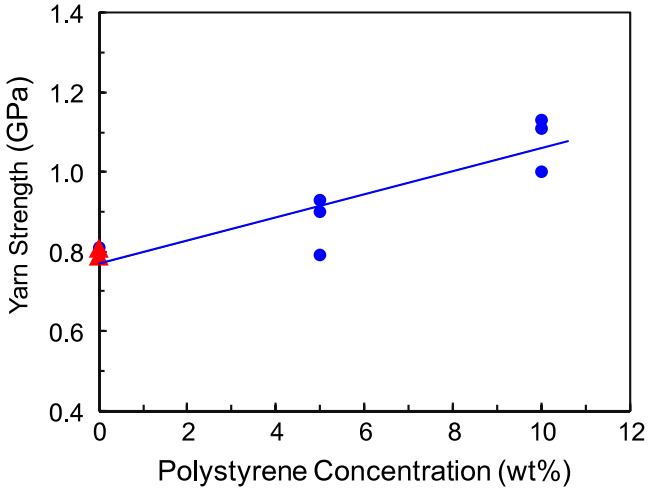

Figure 5. Tensile strength of ∼4.5 μm diameter polystyrene-infiltrated MWNT yarns as a function of the concentration of the polystyrene solution. Closed circles show yarns infiltrated with polystyrene/chloroform solution. Triangles correspond to yarns that have not been solution-treated.

was polystyrene (PS) dissolved in chloroform. Since the PS/chloroform solutions used have low viscosities over a substantial concentration range, we were able to evaluate PS infiltration over this concentration range without encountering the serious problem of polymer overcoating on the yarn surface. Since the tensile strength of our twist-spun yarn increases with decreasing yarn diameter (figure 3), we used small-diameter yarn (4.5 μm diameter) that provided an average tensile strength of 800 MPa. Figure 5 shows the tensile strength of these polystyrene-infiltrated yarns. After infiltration with 10 wt% polystyrene solution, the strength of the thin yarns reached an average value of 1.04 GPa. This corresponds to an increase of around 1.3 times, compared to the untreated thin yarns. The relatively small size of this increase suggests mechanical coupling between nanotube bundles is already large before polymer infiltration.

This strength increase would be most useful if the electrical properties of the CNT yarns remain intact after PS infiltration. As-spun MWNT yarns typically have electrical conductivity in the range of 380–550 S cm^{-1}, but can reach 700 S cm^{-1}. Our results show that the electrical conductivity of twist-spun yarn generally remains unchanged or even slightly increased after PS infiltration. This slight conductivity increase may be largely due to the effect of polymer binding in partial elimination of 'spring-back' (partial reversal of yarn densification at the end of liquid evaporation). These high conductivities result from formation of inter-nanotube electronic connections before polymer infiltration, and contrast with the low electrical conductivities that generally result when nanotubes and polymer are simultaneously co-assembled during solution-based composite yarn spinning [24], which was first demonstrated in the pioneering work of Poulin's group [25] that provided the first practical method for the continuous production of carbon nanotube composite yarns having attractive properties.

Another approach for densifying nanotube yarn is to use false twist, which is much more economical to insert than true twist. In one example (figure 6), 26 000 turns m^{-1} twist was introduced in the clockwise direction to produce a true-twisted yarn, and then the same level of twist is introduced in the counterclockwise direction to produce a false-twisted yarn having an overall level of zero twist. Compared with the highly oriented aerogel, which has a tensile strength of ∼0.2 MPa, the false-twisted yarn has a dramatically increased density and tensile strength (∼113 MPa).

4. Conclusion

In this study, we investigated the effects of processing conditions and nanotube length on the properties of solid-state spun carbon nanotube yarns. The data and analysis indicate that stress transfer between outer and inner walls of individual MWNTs, stress transfer between outer and inner nanotubes in a bundle, and stress transfer between nanotube bundles are the limiting factors for achieving higher strengths for MWNT yarns. Utilizing the understanding, we have improved the engineering mechanical strengths to 800 MPa (1 GPa cm^3 g^{-1} for specific yarn strength) for our solid-state spun MWNT yarns. Average mechanical strengths of 1040 MPa were obtained for PS-infiltrated MWNT yarns and the electrical conductivities of the yarns were as high as 700 S cm^{-1}. The results show that the electrical conductivity of twist-spun yarn generally remains unchanged or slightly increased after PS infiltration. Our experimental results provide a clear path for improving the mechanical strength of nanotube yarns, which involves transitioning from large-diameter MWNTs to single-wall nanotubes or ultra-long few-wall nanotubes that are unbundled or in small bundles.

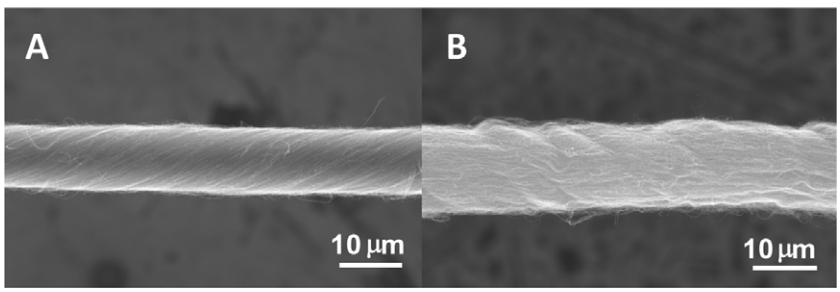

Figure 6. SEM images of (A) true-twisted yarn with 26 000 turns m^{-1} twist and (B) false-twisted yarn obtained by insertion of 26 000 turns m^{-1} twist, followed by removal of this twist by twist insertion in the opposite direction.

Acknowledgments

This work was supported by Air Force Office of Scientific Research grants FA9550-05-C-0088 and FA 9550-09-1-0384, NSF grant DMI-0609115, Office of Naval Research MURI grant N00014-08-1-0654, and the Robert A Welch Foundation grants AT-0029 and AT-1617.

References

[1] Baughman R H, Zakhidov A A and de Heer W A 2002 *Science* **297** 787
[2] Dresselhaus M S, Dresselhaus G and Eklund P C 1996 *Science of Fullerenes and Carbon Nanotubes* (San Diego, CA: Academic)
[3] Rao A M, Richter E, Bandow S, Chase B, Eklund P C, Williams K A, Fang S, Subbaswamy K R, Menon M, Thess A, Smalley R E, Dresselhaus G and Dresselhaus M S 1997 *Science* **297** 187
[4] Yu M-F, Files B S, Arepalli S and Ruoff R S 2000 *Phys. Rev. Lett.* **84** 5552
[5] Walters D A *et al* 1999 *Appl. Phys. Lett.* **74** 3803
[6] Jiang K L, Li Q Q and Fan S S 2002 *Nature* **419** 801
[7] Zhang M, Atkinson K R and Baughman R H 2004 *Science* **306** 1358
[8] Zhang X *et al* 2006 *Adv. Mater.* **18** 1505
[9] Li Q *et al* 2006 *Adv. Mater.* **18** 3160
[10] Zhang X *et al* 2007 *Small* **3** 244
[11] Xiao L *et al* 2008 *Appl. Phys. Lett.* **92** 153108
[12] Zhang S, Zhu L, Minus M L, Chae H G, Jagannathan S, Wong C-P, Kowalik J, Roberson L B and Kumar S 2008 *J. Mater. Sci.* **43** 4356
[13] Nakayama Y 2008 *Japan. J. Appl. Phys.* **47** 8149
[14] Tran C D, Humphries W, Smith S M, Huynh C and Lucas S 2009 *Carbon* **47** 2662
[15] Zhang M, Fang S, Zakhidov A A, Lee S B, Aliev A E, Williams C D, Atkinson K R and Baughman R H 2005 *Science* **309** 1215
[16] Hearle J W S, Grosberg P and Backer S 1969 *Structural Mechanics of Fibers, Yarns, and Fabrics* vol 1 (New York: Wiley)
[17] Ding W, Calabri L, Kohlhaas K M, Chen X, Dikin D A and Ruoff R S 2007 *Exp. Mech.* **47** 25
[18] Yu M F, Yakobson B I and Ruoff R S 2000 *J. Phys. Chem.* B **104** 8764
[19] Hong B H *et al* 2005 *Proc. Natl Acad. Sci. USA* **102** 14155
[20] Zhang M, Fang S, Baughman R H, Zakhidov A A, Atkinson K R, Aliev A E, Li S and Williams C 2007 Fabrication and application of nanofiber ribbons and sheets and twisted and non-twisted nanofiber yarns *Filed PCT Int. Application* CODEN:PIXXD2 WO 2007015710 A2 20070208 p 425
[21] Liu K, Sun Y, Zhou R, Zhu H, Wang J, Liu L, Fan S and Jiang K 2010 *Nanotechnology* **21** 045708
[22] Zhong X H, Li Y L, Liu Y K, Qiao X H, Feng Y, Liang J, Jin J, Zhu L, Hou F and Li J Y 2010 *Adv. Mater.* **22** 692
[23] Koziol K, Vilatela J, Moisala A, Motta M, Cunniff P, Sennett M and Windle A 2007 *Science* **318** 1892
[24] Dalton A B, Collins S, Muñoz E, Razal J M, Ebron V H, Ferraris J P, Coleman J N, Kim B G and Baughman R H 2003 *Nature* **423** 703
[25] Vigolo B *et al* 2000 *Science* **290** 1331